This is a preprint, the final version is subject to change, of the American Mineralogist (MSA)
Cite as Authors (Year) Title. American Mineralogist, in press.
(DOI will not work until issue is live.) DOI: http://dx.doi.org/10.2138/am-2017-5687

Manuscript Number 5687R

Version 3

Bacterially mediated morphogenesis of struvite and its implication for phosphorus recovery

Han Li[1], Qi-Zhi Yao[2*], Sheng-Hui Yu[1], Ya-Rong Huang[1], Xiang-Dong Chen[3], Sheng-Quan Fu[4], Gen-Tao Zhou[1*]

[1] CAS Key Laboratory of Crust-Mantle Materials and Environments, School of Earth and Space Sciences, University of Science and Technology of China, Hefei 230026, P. R. China.

[2] School of Chemistry and Materials Science, University of Science and Technology of China, Hefei 230026, P. R. China.

[3] State Key Laboratory of Virology, College of Life Sciences, Wuhan University, Wuhan 430072, P. R.China

[4] Hefei National Laboratory for Physical Sciences at Microscale, University of Science and Technology of China, Hefei 230026, P. R. China.

● Corresponding author：Prof. Dr. Gen-Tao Zhou

Email: gtzhou@ustc.edu.cn

Tel.: 86 551 63600533

Fax: 86 551 63600533

Abstract

Bacterially mediated struvite usually crystallizes as unusual morphologies. To better understand the relationship between growth habit of struvite and bacterial activity in struvite biomineralization process, *Shewanella oneidensis* MR-1 was selected as a model microbe to induce struvite mineralization in the synthetic sludge liquor. A combination of bacterial and biomimetic mineralization strategies was adopted. Different bacterial components were isolated from the cultures by a set of separation techniques, and used to influence struvite crystallization and growth. The identification and characterization of the mineralized products were done using XRD, FT-IR, FESEM, TG-DTA, XPS, and elemental analysis. Bacterial mineralization experiments demonstrated that *S. oneidensis* MR-1 can not only trigger mineralization and growth of struvite, but also mediate the specific morphogenesis of struvite. Biomimetic mineralization experiments revealed that different bacterial components had different effects on struvite morphology, and low molecular-weight peptides secreted by the bacteria played a dominant role. Current results can provide a deeper insight into bacterially mediated struvite morphogenesis, and be potentially applied to phosphorus and nitrogen recovery from various eutrophic wastewaters.

Keywords: Struvite; biomineralization; morphogenesis; bacteria; extracellular polymeric substances (EPS); low molecular-weight organics

Introduction

Struvite, known as magnesium ammonium phosphate hexahydrate ($MgNH_4PO_4 \cdot 6H_2O$), crystallizes in the orthorhombic system and adopts a series of abiotic morphologies including equant, short prismatic, wedge-shaped, and tabular shapes (Abbona and Boistelle, 1979). Although struvite is not widely found in nature, it has still been discovered in some peculiar environments associated with organic matter decomposition, such as guano deposits, basaltic caves, marshlands, manures, and sediments rich in organic remains (Ben Omar et al., 1998; Sánchez-Román et al., 2007). In recent years, struvite has received increasing attention. On the one hand, struvite is the main component of infectious urinary stones resulting from urinary tract infection by urease-producing bacteria such as *Proteus mirabilis* (e.g., Prywer and Torzewska, 2009, 2010; Prywer et al., 2012; Li et al., 2015). On the other hand, struvite can be potentially used as a fertilizer (Doyle and Parsons, 2002; Le Corre et al., 2009). This makes struvite crystallization and precipitation a new route to phosphorus and nitrogen recovery from wastewater. As such, numerous efforts have been carried out at laboratory, pilot and full-scale to increase yield and lower production costs of struvite (Stratful et al., 2001; Jaffer et al., 2002; de-Bashan and Bashan, 2004; Le Corre et al., 2007; Mehta and Batstone, 2013; Birnhack et al., 2015). Nevertheless, these studies mostly focused on the effects of physicochemical parameters (e.g., pH, mixing energy, temperature, supersaturation level and foreign ions) on struvite precipitation but not the microbial action (Le Corre et al., 2009; Soares et al., 2014).

In fact, there is a close relationship between struvite mineralization and microbial activity. It has been found that many bacterial strains, such as *Proteus mirabilis*, *Myxococcus xanthus*, *Acinetobacter calcoaceticus*, *Bacillus pumilus*, and *Brevibacterium antiquum*, are able to produce struvite crystals in different natural habitats (Rivadeneyra et al., 1992, 1999; Da Silva et al., 2000; Prywer and Torzewska, 2009; Soares et al., 2014; Han et al., 2015). Bacteria isolated from the wastewater treatment plants (WWTPs) can also precipitate struvite (Rivadeneyra et al., 2014; Gonzalez-Martinez et al., 2015). Bacterial production of struvite results from their metabolism of nitrogenous compounds accompanied with ammonium release and the consequent pH increase (Sánchez-Román et al., 2007; Sinha et al., 2014). The

presence of bacterial cells or certain parts of the cell is also necessary to act as heterogeneous nuclei for struvite crystallization (González-Muñoz et al., 1996; Ben Omar et al., 1998; Sinha et al., 2014). Meanwhile, bacteria are able to effect and modify struvite morphology, and a series of different morphologies of struvite were observed in the bacterial mineralization experiments (Prywer and Torzewska, 2009, 2010; Prywer et al., 2012; Sadowski et al.,2014; Sinha et al., 2014). For example, the coffin-like, X-shaped and dendritic struvite crystals were obtained in the presence of *Proteus* bacteria (Prywer and Torzewska, 2009, 2010; Prywer et al., 2012), whereas the prismatic struvite crystals were produced by a metallophilic bacterium *Enterobacter sp.* (Sinha et al., 2014). Moreover, Sadowski et al. (2014) reported that the struvite mineralized by bacterium *Proteus mirabilis* has more regular habit than that without bacteria. These results confirmed the ability of bacteria to mediate morphogenesis of struvite. However, the precise mechanisms are not fully understood, and the specific bacterial components responsible for morphological modification of struvite, as pointed out by Prywer et al. (2012), remain to be determined.

As for the struvite recovery, the shape and size must be validly controlled during struvite crystallization in wastewater from a process engineering viewpoint, and the tabular struvite is suggested to be the most desirable due to its more uniform shape and lower likelihood of breaking into smaller fragments (Le Corre et al., 2009; Mehta and Batstone, 2013). As the most adequate medium for struvite formation and recovery (de-Bashan and Bashan, 2004; Birnhack et al., 2015), supernatant of sludge has quite high bacterial abundances (Kwon et al., 2010; Yang et al., 2011; Ibarbalz et al., 2013). This necessitates understanding the relationship between struvite morphology and bacteria in the struvite recovery process. Moreover, wastewater tends to be deficient in magnesium ions (de-Bashan and Bashan, 2004), and the addition of Mg(II) is indispensable to phosphorous recovery from wastewater. The pH adjustment is also needed to reach the appropriate pHs for struvite crystallization. Therefore, the dosage of Mg(II) and/or pH adjustment will increase the recovery cost from wastewater by the abiotic crystallization process (Jaffer et al., 2002; Le Corre et al., 2009). This significantly limits its application at full scale. In contrast, the bacterial metabolic activity can generate the necessary alkaline environment for struvite precipitation, and thus absolving utilization of the base (Sánchez-Román et al., 2007; Rivadeneyra et al., 2014; Sinha et al.,

2014). Therefore, the bacterial mineralization of struvite was regarded as a promising strategy to recover phosphorus and nitrogen from wastewater (Sinha et al., 2014; Soares et al., 2014). Despite all that, there remains a dearth of research examining the bacterial impact on the struvite morphogenesis.

The aim of this study was to investigate the effect of bacterial cells (*Shewanella oneidensis* MR-1) and different metabolites on the morphogenesis of struvite in the synthetic sludge liquor. An in situ biomineralization and biomimetic mineralization were carried out, respectively. The different bacterial components separated from the cultures were used to influence struvite growth. As a consequence, the ability of *S. oneidensis* MR-1 to mineralize struvite and mediate struvite morphogenesis was examined, and a plausible mechanism for the morphogenesis of bio-struvite was proposed. This may prove useful for a better understanding of biomineralization and the development of struvite recovery technique.

Materials and methods

Materials

All starting inorganic reagents are of analytical grade and purchased from Sinopharm Chemical Reagent Co., Ltd. The tryptone and yeast extract are of biotech grade and purchased from Oxoid Ltd. Deionized water was used in all of the experiments.

Bacterial strain

Shewanella oneidensis MR-1 (ATCC 700550) was used in present study. The genus *Shewanella* is widely distributed in nature, especially associated with aquatic and marine environments (Xiao et al., 2007; Zhao et al., 2010). Some strains such as *S. putrefaciens*, *S. decolorationis* and *S. oneidensis* were also found in the wastewater and activated sludge of the WWTPs (Kämpfer et al., 1996; Xu et al., 2005; Khalid et al., 2008; Wu et al., 2009). Here, *S. oneidensis* MR-1 was chosen as a model organism because of its metabolic versatility and sequenced and annotated genome (Bretschger et al., 2007).

Bacteria cultivation and EPS extraction

Shewanella oneidensis MR-1 was inoculated into 100 mL of sterilized Luria-Bertani (LB)

137 medium (10 g/L tryptone, 5 g/L yeast extract, 5 g/L NaCl) by adding 0.1 mL of the seed
138 culture. Strain MR-1 was then cultured aerobically for 24 h at 30 °C with constant shaking
139 (200 rpm) up to a cell density of 6×10^9 CFU per mL. The final liquid culture containing *S.*
140 *oneidensis* was centrifuged at 4000 × g for 20 min at 4 °C to concentrate the bacterial cells.
141 The harvested cells were washed three times with 0.5% (w/w) NaCl solution to remove
142 residual growth medium. The resultant supernatants were filtered through 0.22 μm cellulose
143 acetate membranes to eliminate any remaining cell debris. A portion of the unseparated liquid
144 culture, the filtered supernatant, and the harvested native cells were used in the following
145 biomimetic mineralization experiments.

146 For the separation of soluble extracellular polymeric substances (SEPS), the
147 ultrafiltration device with 1000 NMWL (Nominal Molecular Weight Limit) polyethersulfone
148 ultrafiltration membrane (Millipore Corporation, U.S.) was used to separate the low
149 molecular-weight (LMW) (< 1000 Da) and high-molecular weight compounds from the
150 supernatants (Wang et al., 2012). After ultrafiltration, the high-molecular weight compounds
151 were washed twice with deionized water in the same ultrafiltration device, and denoted as
152 SEPS. The filtrate with LMW component was also kept for the next biomimetic
153 mineralization experiments.

154 For the extraction of bound EPS (BEPS) with bacterial cells, a cation exchange resin
155 (CER) technique (Dowex Marathon C, 20-50 mesh, sodium form, Sigma-Aldrich 91973) was
156 used (Sheng et al., 2008). The washed cell pellets were resuspended in 0.5% NaCl solution,
157 followed by an addition of 30 g CER. After the suspension was stirred for 12 h at 200 rpm and
158 4 °C, the CER was removed by settlement. Subsequently, the solution was centrifuged at
159 10,000× g for 30 min to isolate the cell pellets without EPS (denoted as EPS-free cells or bare
160 cells) and supernatant. The EPS-free cells were washed twice with 0.5% NaCl solution and
161 resuspended for further use. The supernatant was further filtered through 0.22 μm cellulose
162 acetate membrane to obtain the filtrate (denoted as BEPS).
163

164 **Bacterial mineralization**

165 Three kinds of culture media (M-1, M-2 and M-3) were used, and corresponding
166 compositions are listed in Table 1. Medium M-1 is a composition of LB medium and the

synthetic sludge liquor, which was prepared according to the values reported by Doyle et al. (2000). In media M-2 and M-3, no ammonium and/or phosphate ions was added. To make these culture media, 5 mL of deionized water dissolved with 0.0895 g $MgCl_2 \cdot 6H_2O$ was added into 100 mL sterilized LB medium by filtration sterilization through 0.22 μm cellulose acetate membranes. After that, 5 mL of deionized water solution with 0.0506 g $NH_4H_2PO_4$ and 0.0471 g NH_4Cl was added into the LB medium to obtain culture medium M-1, while the media M-2 and M-3 were obtained by adding 5 mL of solution with 0.0686 g $NaH_2PO_4 \cdot 2H_2O$ and only 5 mL of deionized water, respectively. Initial pH (pH_i) 7.0 was used in all three media in order to avoid any precipitation before inoculation. 110 mL of each medium was aerobically inoculated by adding 0.1 mL of the seed culture at 30 °C and 200 rpm. The cultures were checked periodically for identifying the precipitate appearance. Comparative tests without inoculation were also conducted. All experiments were performed in triplicate. At the end of the incubation period the final pH was measured, and the mineral precipitates were harvested by settlement. The products were washed with absolute alcohol three times, and dried in vacuum at room temperature for 48 h.

Biomimetic mineralization

The biomimetic crystallization experiments were also conducted in a dynamic environment at room temperature. A synthetic sludge liquor was used for crystallization according to the values reported by Doyle et al. (2000). In a typical synthesis, 0.0407 g (0.2 mmol) of $MgCl_2 \cdot 6H_2O$ was dissolved in 2.5 mL of deionized water under vigorous stirring to form solution A. Then, 0.0214 g (0.4 mmol) of NH_4Cl and 0.023 g (0.2 mmol) of $NH_4H_2PO_4$ were dissolved in 2.5 mL of deionized water to form solution B. Solution C is a series of 45 mL solutions with different bacterial components (Table 2), which were separated from 45 mL of culture according to the procedures described above. The pH of solution C was adjusted to pH 6.0 using 0.5 M HCl solution. After that, solution A and B were introduced into solution C under continuous stirring to obtain a homogeneous liquor, and the final concentrations of Mg^{2+}, PO_4^{3-}, and NH_4^+ were 4 mmol/L, 4 mmol/L, and 12 mmol/L, respectively. Then pH of the liquor was adjusted to 9.0 using 0.5 M NaOH. The beaker with reactants was covered with parafilm, and stirred for 3 h at 360 rpm on a magnetic stirrer to precipitate struvite. All

experiments were run in triplicate. In control experiments without bacterial components, the solution C was 45 mL of deionized water, 0.5% NaCl solution, or uninoculated culture medium, respectively. To avoid microbial contamination, the experimental equipment and solutions were UV-sterilized for 30 minutes in a clean bench prior to the experiments, and the experiments were also conducted in a clean bench. Finally, the precipitation products were isolated by centrifugation (1400 g for 3 min) and washed and dried by the procedures described in Section "Bacterial mineralization".

Sample analysis

X-ray diffraction (XRD) analysis of the samples was conducted on a Japan MapAHF X-ray diffractometer using Cu Kα irradiation (λ = 0.154056 nm). Morphology of the precipitates was studied using a JEOL JSM-6700F field emission scanning electron microscope (FESEM). Infrared (IR) spectrum analysis was carried out on a Nicolet 8700 FT-IR spectrophotometer on KBr pellets. Thermogravimetric and differential thermal analyses (TG-DTA) were conducted employing a SDT Q600 thermal analyzer (TA, USA) with a heating rate of 10°C /min from room temperature to 800°C under air gas flow. X-ray photoelectron spectra (XPS) were obtained on a Thermo ESCALAB 250 X-ray photoelectron spectrometer using Al Kα radiation. The carbon, nitrogen, and hydrogen contents of the sample was determined by a Vario EL III elemental analyzer (Elementar, German). The amino acid contents were analyzed by a L-8800 amino acid analyzer (Hitachi, Japan). The inorganic phosphate concentration was analyzed by ion chromatograph (IC, Dionex ICS-3000).

Results and discussion

Bacterial mineralization experiments were first conducted to understand the ability of *S. oneidensis* MR-1 to produce struvite and the bacterial effect on struvite morphogenesis. After 3 d of incubation, white precipitates were obtained in all three inoculated media (M-1, M-2 and M-3). The XRD analyses confirmed that these precipitates were pure orthorhombic struvite with space group $Pmn2_1$, and the representative XRD pattern was shown in Figure 1a. However, no precipitate was found in the comparative experiments without bacteria,

226 indicating that *S. oneidensis* MR-1 was able to facilitate struvite formation. The pH
227 measurements showed that the pHs in the three inoculated media rose from 7.0 to around 9.0,
228 while the pH of the control almost remained unchanged. This indicated that bacterial
229 metabolism raised the pH, and thus promoted struvite formation. Meanwhile, almost the same
230 amount of struvite was harvested in the three different media, and the transformation
231 efficiency of magnesium ranged from 68.0% to 70.5% (Table 1). However, unlike medium
232 M-1, there was no addition of ammonium and/or phosphate ions in the initial media M-2 and
233 M-3 (Table 1). This indicated that the metabolism of *S. oneidensis* MR-1 could produce a
234 large amount of ammonium and phosphate, leading to struvite precipitation. To further
235 confirm the conclusion, the concentration of inorganic phosphate in the uninoculated culture
236 medium or the final culture supernatant after inoculation for 3 d was measured by ion
237 chromatograph (IC), and corresponding phosphate concentrations were 60.90 μg/mL (1.97
238 mM) and 176.24 μg/mL (5.69 mM), respectively. Therefore, the strain MR-1 can convert
239 organophosphorus into inorganic phosphate by their metabolic activity. This similar
240 metabolism process had been found in other bacterial strains, such as *Enterobacter sp.* and
241 *Chromohalobacter marismortui* (Rivadeneyra et al., 2006; Sinha et al., 2014). The release of
242 ammonium and phosphate may result from degradation of peptones and yeast extract in the
243 medium, as reported by several researchers (Sánchez-Román et al., 2007; González-Muñoz et
244 al., 2008; Rivadeneyra et al., 2014; Sinha et al., 2014).

245 In a word, the bacterial in situ mineralization experiments revealed that metabolism of *S.*
246 *oneidensis* MR-1 could efficiently promote struvite formation by arising pH and secreting
247 ammonium and phosphate into the culture medium. Hence, *S. oneidensis* MR-1 may play an
248 important role in the struvite precipitation in aquatic environments including the sludge liquor.
249 Moreover, the FESEM observation (e.g., Figure 1b) shows that the obtained struvite crystals
250 possessed coffin-like habit, which exhibited typical hemimorphic morphology and can be
251 described as a crystallographic combination composed of the {00-1} pedion, the {101},
252 {-101}, {012} and {0-12} domes (inset in Figure 1b). This is significantly different from the
253 abiogenic equant, short prismatic, wedge-like, and tabular morphologies (Abbona and
254 Boistelle, 1979). The similar coffin-like morphology has also been found during the
255 mineralization of struvite with *Proteus mirabilis* in artificial urine (Prywer and Torzewska,

256 2009, 2010; Prywer et al., 2012). It appears that *S. oneidensis* MR-1 can effect and modify
257 morphogenesis of struvite. In order to understand the precise details, some biomimetic
258 mineralization experiments with different bacterial components were also carried out.

259 Figure 2a depicts the typical FESEM image of the product obtained after 3 h of
260 mineralization in the presence of unseparated liquid culture, exhibiting the presence of a large
261 number of coffin-like crystals with a length of ca. 16 μm and a width of ca. 13 μm (Figure 2a),
262 which are similar to those obtained in the bacterial mineralization experiments (e.g., Figure
263 1b). The XRD analysis confirmed them as pure struvite (Figure 3a). However, such habit did
264 not appear in the control experiments with deionized water, 0.5% NaCl solution, or
265 uninoculated culture medium. Only long tabular crystals were harvested in the deionized
266 water or 0.5% NaCl solution (Figure 2b and 2c), and the XRD analyses also identified them
267 as pure struvite (Figure 3b). This precludes that NaCl in the liquid culture contributed to the
268 formation of coffin-like habit. Interestingly, struvite with trapezoidal shape was obtained in
269 the uninoculated culture medium (Figure 2d and 3c), indicating that some organic matters
270 from initial culture medium had an influence on struvite morphology. However, the marked
271 morphologic contrast of the struvite crystals obtained from the bacterial culture and
272 uninoculated culture medium revealed that bacterial activity could significantly influence
273 struvite crystallization and morphogenesis.

274 In order to understand the mediation of different components in unseparated liquid
275 culture on struvite morphology, the culture was separated into two parts, i.e., supernatant and
276 bacterial cells (e.g., Table 2). The effect of the supernatant and bacterial cells on struvite
277 morphogenesis was then investigated under the similar mimetic conditions, respectively. After
278 3 h of mineralization, only long tabular struvite crystals were obtained in the solution bearing
279 bacterial cells (Figure 2e and 3d). This morphology was similar to that obtained in the
280 deionized water (Figure 2b) or 0.5% NaCl solution (Figure 2c), indicating that bacterial cells
281 had little influence on struvite morphogenesis. However, the struvite crystallized from the
282 supernatant (Figure 2f and 3e) almost exhibited the same coffin-like habit as that from the
283 unseparated liquid culture (Figure 2a), indicating that the bacterial components in the
284 supernatant should be responsible for coffin-like habit of struvite.

285 It is well known that bacterial supernatant contains various bacterial metabolites

286 including proteins and peptides, small molecular amino acids, etc.(e.g., Braissant et al., 2003;
287 Juang et al., 2008; Dupraz, et al., 2009; Prywer et al., 2012). Moreover, numerous
288 investigations have shown that these biomolecules can influence crystallization and specific
289 morphogenesis of biogenic minerals including struvite (Asakura et al. 1998; Taller et al., 2007;
290 Song et al., 2014; Li et al., 2015). For example, osteopontin (urinary protein) was believed to
291 be responsible for the dumbbell-like calcium oxalate monohydrate crystals in human urine
292 (Taller et al., 2007). Peptides with defined secondary structure were reported to exert
293 significant control over the morphology of magnetite and calcite crystals (DeOliveira and
294 Laursen, 1997; Arakaki et al., 2010). Small molecules citric acid and succinic acid could also
295 change the struvite morphology from regular needle-shape to angular-shaped and irregular
296 block, whereas macromolecules calprotectin (another urinary protein) led to the formation of
297 the X-shaped struvite (Asakura et al. 1998; Song et al., 2014). We recently found that
298 polyaspartic acid can dominate the formation of arrowhead-shaped and X-shaped struvite (Li
299 et al., 2015). These results indicated that the metabolites secreted by the strain MR-1 can
300 potentially exert different controls over the struvite morphogenesis. Therefore, the supernatant
301 was further separated into low molecular-weight (LMW) (< 1000 Da) and macromolecule
302 (e.g., SEPS) components by ultrafiltration, and the effects of the different components on
303 struvite morphology were tested. Our results showed that in the presence of LMW component,
304 a 3 h of mineralization led to the crystals with coffin-like profile (Figure 4a), whereas
305 prismatic crystals were obtained with the SEPS (Figure 4b). The XRD analyses identified
306 them as struvite, as shown in Figure S1a and b. Hence, it can be easily concluded that the
307 LMW component in the bacterial supernatant mediated the formation of the coffin-like
308 struvite. The influence of the LMW component on struvite can be achieved through the
309 preferential binding of their functional groups with some specific faces of struvite crystals.
310 Therefore, the LMW component should exert crucial control on the formation of the
311 coffin-like struvite during the bacterial mineralization.

312 To further understand the mediation of the LMW component on struvite morphogenesis,
313 a series of analytical techniques including FT-IR, TG-DTA and XPS were used to characterize
314 the coffin-like struvite obtained with the LMW component. The FT-IR and TG-DTA analyses
315 showed that the struvite harvested from the LMW component solution was almost pure, and

316 no organic impurities were detected (Figures S2a and S3a). However, the elemental analysis
317 showed that the carbon in the struvite accounts for about 0.94 wt % (Table 3), indicating that
318 some organic molecules should be associated with the coffin-like struvite crystals. As the
319 content of the organics is low, they were not detected by FT-IR and TG-DTA analyses.

320 The surface composition of the struvite was further determined by XPS over the energy
321 range of 0-1350 eV. As depicted in Figure 5a, the core level peaks were O 1s (531.0 eV), P 1p
322 (131.9 eV), Mg 1s (1303.4 eV), C 1s (285.1 eV), and N 1s (399.5 eV). The mass fractions of
323 O, P, Mg, C and N were estimated to be 38.84%, 30.33%, 17.26%, 9.97%, and 3.60%,
324 respectively. It is worth noticing that the mass fraction of C detected by XPS (9.97%) is much
325 higher than that of the elemental analyzer (0.94%), indicating that much more organics were
326 concentrated on the surfaces of struvite, and it is the organic molecules that play an important
327 role in the struvite morphogenesis by their surface binding. To better clarify the organic
328 molecules involved in the struvite morphogenesis, high resolution scans of C 1s, O 1s, and N
329 1s were deconvoluted, and the corresponding functional groups were recognized. Figure 5b-d
330 depicts the presence of five C (1s), two O (1s), and two N (1s). Table S1 in Supporting
331 Information lists the assignment and quantification of these functional groups. In a word, the
332 XPS results could assign the LMW organics anchored on the surfaces of struvite crystals as
333 the compounds enriched in carboxyl and amine/amide groups such as amino acids or peptides.
334 Furthermore, the amino acids in LMW organics solution and uninoculated culture medium
335 were analyzed, respectively, as listed in Table S2. The results revealed that there are 17 free
336 amino acids in either the uninoculated culture medium or the supernatant with LMW
337 component, and the majority amino acids remarkably decreased in content after a 24 h of
338 culture, indicating that bacterial metabolism consumed these amino acids. Meanwhile, it is
339 worth noticing that some amino acids such as proline, tyrosine and alanine, obviously
340 increased in the LMW supernatant (e.g., Table S2) indicating that these amino acids may
341 dominate the morphogenesis of coffin-like struvite. However, the biomimetic mineralization
342 experiments with proline, tyrosine, alanine, or their combinations, only resulted in long
343 tabular crystals (data not shown), indicating that the small molecule amino acids had little
344 influence on the struvite morphogenesis. In fact, our previous study has demonstrated that
345 polypeptide polyaspartic acid could regulate the morphogenesis of struvite by their anchoring

346 with the specific crystal faces of struvite, while its monomer aspartic acid almost did not exert
347 the resemblant effect (Li et al., 2015). Similar phenomena have been found in other minerals,
348 such as calcium oxalate monohydrate and calcium hydrogenphosphate dihydrate (Sikirić et al.
349 2000, Guo et al. 2002). These indicated that binding of the biomolecules with the specific
350 crystal faces may not occur in proportion to the abundance of the functional groups. This
351 could be attributed to stereochemical distinctions (e.g., chain length and spatial conformation)
352 between polypeptide and its monomer (e.g., Braissant et al., 2003; Li et al., 2015). Combined
353 with the XPS results, it can be believed that the LMW peptides are responsible for the
354 formation of coffin-like biogenic struvite.

355 In fact, coffin-like struvite had been reported by several studies involved in bacterial
356 mineralization experiments and coffin-like habit is typical hemimorphic morphology (Prywer
357 and Torzewska, 2009, 2010; Prywer et al., 2012). In the basic crystal morphology of struvite,
358 the (001) face is terminated by NH_4^+ groups while the (00-1) face is terminated by PO_4^{3-} and
359 $Mg(H_2O)_6^{2+}$ groups (Abbona et al., 1984). Therefore, Prywer et al. (2012) pointed out that
360 bacterial components with anionic character are easy to bind Mg^{2+} ions on the (00-1) face and
361 thus slow down its growth. The (001) face grew freely and fast. According to crystal growth
362 theory, the exposed crystal faces are usually those faces that grow slowly, and the less
363 exposed or vanishing faces are fast growing faces. Hence, the (001) face is much smaller than
364 the (00-1) face. In this way, coffin-like habit was developed. Prywer et al. (2012) also
365 speculated that the bacterial components responsible for preferential binding with (00-1) were
366 polysaccharides, which represent the outermost structures of *P. mirabilis* cell. However, this
367 hypothesis remains to be confirmed, and our results showed that the LMW organics such as
368 peptides in the supernatant played a major role in the formation of hemimorphic struvite. That
369 is, LMW peptide molecules with negatively charged carboxyl group preferentially binding to
370 (00-1) face of struvite result in an enhanced expression of the (00-1) face, and thus the
371 formation of coffin-like struvite.

372 Although our experimental results revealed that the bacterial cells themselves could not
373 lead to coffin-like struvite (e.g., Fig. 2e), a number of studies showed that the outer structures
374 of microbial cells such as the cyanobacterial S-layer have already been recognized as the main
375 crystalline biostructure acting as a nucleus for mineral growth or as a morphological regulator

(e.g., Schultze-Lam et al. 1992; Braissant et al., 2003; Ercole et al., 2007; Tourney and Ngwenya, 2009). Hence, the native cells were specially disassociated into BEPS and EPS-free cells (bare cell) to investigate their individual mineralization functions. Our results showed that in the presence of EPS-free cells, a mass of long tabular struvite crystals were harvested with 3 h of mineralization (Figure 6a), resembling the features encountered in the native cells (Figure 2e). Nevertheless, in the presence of the BEPS, almost all of crystals exhibited the truncated tabular-like structures (Figure 6b), and the XRD results showed that they are struvite (Figure S4). Such truncated tabular morphology was different from the long tabular (from bare cells, Figure 6a) and the prismatic (from SEPS, Figure 4b) morphologies, indicating that the BEPS could modify struvite morphology, and these two kinds of EPS molecules exerted different effects on the growth of struvite crystals. This can be attributed to the differing chemical properties between BEPS and SEPS. In general, both SEPS and BEPS are mainly composed of polysaccharides and proteins, and the SEPS has higher concentration of polysaccharides than the BEPS (Comte et al., 2006; Pan et al., 2010). Moreover, Ercole et al. (2007) have also confirmed that the SEPS and BEPS isolated from *Bacillus firmus* or *Bacillus sphaericus* led to the different morphologies of calcite. It appears that the SEPS and BEPS with different biochemical composition have different controls on the growth and morphogenesis of struvite. This point should be of significance in the interpretation of struvite mineralogy in the struvite recovery process.

Implications

Bacterially induced and mediated mineralization processes are widespread in nature, leading to precipitation of a variety of minerals, such as carbonates, phosphates, sulphides, oxides and silicates (e.g., Ehrlich, 2002). To understand the biomineralization mechanisms, live cultures of various bacterial strains were often used (e.g., Da Silva et al., 2000; Rivadeneyra et al., 2006; Sánchez-Román et al., 2007; Dupraz, et al., 2009; Prywer and Torzewska, 2009, 2010; Prywer et al., 2012; Sinha et al., 2014). However, because of the complexity of the bacterial system, bacterial cells and metabolites, even the ingredients of culture media may all affect the mineralization processes (e.g., Tourney and Ngwenya, 2009;

Prywer et al., 2012; Zhang et al., 2015). This leads to the poor recognization to the components responsible for morphogenesis and/or polymorph selection of biominerals. In this study, by using a series of separation techniques and the combination of bacterial and biomimetic mineralization strategies, different bacterial components such as native cells, EPS-free cells, BEPS, SEPS, and LMW components were isolated from the bacterial cultures, and used to influence struvite mineralization. Our results revealed that different bacterial components had different effects on struvite morphology, and low molecular-weight peptides secreted by the bacteria dominate the struvite morphogenesis. This can not only give a new insight into struvite biomineralization, but also provides a potential opportunity to elucidate the biomineralization mechanisms of other minerals.

Moreover, struvite crystallization has been the subject of considerable investigations because it offers a new route to recover phosphorus and nitrogen from wastewater (e.g., Doyle and Parsons, 2002; Le Corre et al., 2009). As bacteria can facilitate struvite mineralization by metabolic activity (e.g., Sánchez-Román et al., 2007; González-Muñoz et al., 2008; Rivadeneyra et al., 2014; Sinha et al., 2014), this will help to reduce the cost to produce struvite. Hence, bacterially induced mineralization of struvite has recently been regarded as a more promising route than the abiotic crystallization (Sinha et al., 2014; Soares et al., 2014). Our experimental results revealed that *S. oneidensis* MR-1 was able to produce struvite crystals in the synthetic medium. Considering the presence of bacterium *S. oneidensis* in wastewater (Wu et al., 2009), it will be potentially feasible to employ strain MR-1 for struvite recovery from wastewaters. Meanwhile, strain MR-1 can effectively mineralized over 70% of the magnesium into struvite. This is much higher than the bacterium *Enterobacter sp.* EMB19 with a mineralization efficiency 20% (Sinha et al., 2014). The high utility of magnesium will significantly cut down the cost because the addition of magnesium salt is another principal charge of struvite production. Furthermore, almost same amounts of struvite were harvested in media without addition of ammonium and/or phosphate ions (M-1 and M-3), indicating that strain MR-1 was able to directly transform organophosphorus and organic nitrogen into struvite. This will promote a combination of nitrogen and phosphorus removal and struvite crystallization. In a word, strain MR-1 can not only act as an ideal candidate for bacterial mineralization of struvite from wastewaters but also as a scavenger for eutrophic waters. Our

435 results also showed that *S. oneidensis* MR-1 was able to mediate struvite morphogenesis and
436 different bacterial components had different influence on struvite morphology. This will help
437 to direct controllable crystallization of the recovered struvite.
438

439 ## Acknowledgements

440 This work was partially supported by the Chinese Ministry of Science and Technology (No.
441 2014CB846003), the Natural Science Foundation of China (Nos. 41672034, 41372053), the
442 Specialized Research Fund for the Doctoral Program of Higher Education (No.
443 20133402130007), and the Fundamental Research Funds for the Central Universities (No.
444 WK6030000002).
445

References

Abbona, F., and Boistelle, R. (1979) Growth morphology and crystal habit of struvite crystals ($MgNH_4PO_4 \cdot 6H_2O$). Journal of Crystal Growth, 46, 339-354.

Abbona, F., Calleri, M., and Ivaldi, G. (1984) Synthetic struvite, $MgNH_4PO_4 \cdot 6H_2O$ - correct polarity and surface-features of some complementary forms. Acta Crystallographica Section B-Structural Science, 40, 223-227.

Arakaki, A., Masuda, F., Amemiya, Y., Tanaka, T., and Matsunaga, T. (2010) Control of the morphology and size of magnetite particles with peptides mimicking the Mms6 protein from magnetotactic bacteria. Journal of Colloid and Interface Science, 343, 65-70.

Asakura, H., Selengut, J.D., Orme-Johnson, W.H., and Dretler, S.P. (1998) The effect of calprotectin on the nucleation and growth of struvite crystals as assayed by light microscopy in real-time. Journal of Urology, 159, 1384-1389.

Ben Omar, N., Gonzalez-Munoz, M.T., and Penalver, J.M.A. (1998) Struvite crystallization on *Myxococcus* cells. Chemosphere, 36, 475-481.

Birnhack, L., Nir, O., Telzhenski, M., and Lahav, O. (2015) A new algorithm for design, operation and cost assessment of struvite ($MgNH_4PO_4$) precipitation processes. Environmental Technology, 36, 1892-1901.

Braissant, O., Cailleau, G., Dupraz, C., and Verrecchia, A.P. (2003) Bacterially induced mineralization of calcium carbonate in terrestrial environments: The role of exopolysaccharides and amino acids. Journal of Sedimentary Research, 73, 485-490.

Bretschger, O., Obraztsova, A., Sturm, C.A., Chang, I.S., Gorby, Y.A., Reed, S.B., Culley, D.E., Reardon, C.L., Barua, S., Romine, M.F., Zhou, J., Beliaev, A.S., Bouhenni, R., Saffarini, D., Mansfeld, F., Kim, B.H., Fredrickson, J.K., and Nealson, K.H. (2007) Current production and metal oxide reduction by *Shewanella oneidensis* MR-1 wild type and mutants. Applied and Environmental Microbiology, 73, 7003-7012.

Comte, S., Gulbaud, G., and Baudu, M. (2006) Biosorption properties of extracellular polymeric substances (EPS) resulting from activated sludge according to their type: Soluble or bound. Process Biochemistry, 41, 815-823.

Da Silva, S., Bernet, N., Delgenes, J.P., and Moletta, R. (2000) Effect of culture conditions on

the formation of struvite by *Myxococcus xanthus*. Chemosphere, 40, 1289-1296.

de-Bashan, L.E., and Bashan, Y. (2004) Recent advances in removing phosphorus from wastewater and its future use as fertilizer (1997-2003). Water Research, 38, 4222-4246.

DeOliveira, D.B., and Laursen, R.A. (1997) Control of calcite crystal morphology by a peptide designed to bind to a specific surface. Journal of the American Chemical Society, 119, 10627-10631.

Doyle, J.D., and Parsons, S.A. (2002) Struvite formation, control and recovery. Water Research, 36, 3925-3940.

Doyle, J.D., Philp, R., Churchley, J., and Parsons, S.A. (2000) Analysis of struvite precipitation in real and synthetic liquors. Process Safety and Environmental Protection, 78, 480-488.

Dupraz, C., Reid, R.P., Braissant, O., Decho, A.W., Norman, R.S., and Visscher, P.T. (2009) Processes of carbonate precipitation in modern microbial mats. Earth-Science Reviews, 96, 141-162.

Ehrlich, H.L. (2002) Geomicrobiology, 4th ed., 768 p. Marcel Dekker, Inc, New York.

Ercole, C., Cacchio, P., Botta, A.L., Centi, V., and Lepidi, A. (2007) Bacterially induced mineralization of calcium carbonate: The role of exopolysaccharides and capsular polysaccharides. Microscopy and Microanalysis, 13, 42-50.

Gonzalez-Martinez, A., Leyva-Diaz, J.C., Rodriguez-Sanchez, A., Munoz-Palazon, B., Rivadeneyra, A., Poyatos, J.M., Rivadeneyra, M.A., and Martinez-Toledo, M.V. (2015) Isolation and metagenomic characterization of bacteria associated with calcium carbonate and struvite precipitation in a pure moving bed biofilm reactor-membrane bioreactor. Biofouling, 31, 333-348.

González-Muñoz, M.T., Ben Omar, N., Martinez-Canamero, M., Rodriguez-Gallego, M., Galindo, A.L., and Arias, J.M. (1996) Struvite and calcite crystallization induced by cellular membranes of *Myxococcus xanthus*. Journal of Crystal Growth, 163, 434-439.

González-Muñoz, M.T., De Linares, C., Martinez-Ruiz, F., Morcillo, F., Martin-Ramos, D., and Arias, J.M. (2008) Ca-Mg kutnahorite and struvite production by *Idiomarina* strains at modern seawater salinities. Chemosphere, 72, 465-472.

Guo, S.W., Ward, M.D., and Wesson, J.A. (2002) Direct visualization of calcium oxalate

505 monohydrate crystallization and dissolution with atomic force microscopy and the role
506 of polymeric additives. Langmuir, 18, 4284-4291.
507 Han, Z.Z., Zhao, Y.Y., Yan, H.X., Zhao, H., Han, M., Sun, B., Sun, X.Y., Hou, F.F., Sun, H.,
508 Han, L., Sun, Y.B., Wang, J., Li, H., Wang, Y.Q., and Du, H. (2015) Struvite precipitation
509 induced by a novel sulfate-reducing bacterium *Acinetobacter calcoaceticus* SRB4
510 isolated from river sediment. Geomicrobiology Journal, 32, 868-877.
511 Ibarbalz, F.M., Figuerola, E.L.M., and Erijman, L. (2013) Industrial activated sludge exhibit
512 unique bacterial community composition at high taxonomic ranks. Water Research, 47,
513 3854-3864.
514 Jaffer, Y., Clark, T.A., Pearce, P., and Parsons, S.A. (2002) Potential phosphorus recovery by
515 struvite formation. Water Research, 36, 1834-1842.
516 Juang, R.S., Chen, H.L., and Chen, Y.S. (2008) Resistance-in-series analysis in cross-flow
517 ultrafiltration of fermentation broths of *Bacillus subtilis* culture. Journal of Membrane
518 Science, 323, 193-200.
519 Kämpfer, P., Erhart, R., Beimfohr, C., Bohringer, J., Wagner, M., and Amann, R. (1996)
520 Characterization of bacterial communities from activated sludge: Culture-dependent
521 numerical identification versus in situ identification using group- and genus-specific
522 rRNA-targeted oligonucleotide probes. Microbial Ecology, 32, 101-121.
523 Khalid, A., Arshad, M., and Crowley, D.E. (2008) Accelerated decolorization of structurally
524 different azo dyes by newly isolated bacterial strains. Applied Microbiology and
525 Biotechnology, 78, 361-369.
526 Kwon, S., Kim, T.S., Yu, G.H., Jung, J.H., and Park, H.D. (2010) Bacterial community
527 composition and diversity of a full-scale integrated fixed-film activated sludge system as
528 investigated by pyrosequencing. Journal of Microbiology and Biotechnology, 20,
529 1717-1723.
530 Le Corre, K.S., Valsami-Jones, E., Hobbs, P., Jefferson, B., and Parsons, S.A. (2007)
531 Agglomeration of struvite crystals. Water Research, 41, 419-425.
532 Le Corre, K.S., Valsami-Jones, E., Hobbs, P., and Parsons, S.A. (2009) Phosphorus recovery
533 from wastewater by struvite crystallization: A review. Critical Reviews in Environmental
534 Science and Technology, 39, 433-477.

Li, H., Yao, Q.Z., Wang, Y.Y., Li, Y.L., and Zhou, G.T. (2015) Biomimetic synthesis of struvite with biogenic morphology and implication for pathological biomineralization. Scientific Reports, 5, 7718.

Mehta, C.M., and Batstone, D.J. (2013) Nucleation and growth kinetics of struvite crystallization. Water Research, 47, 2890-2900.

Pan, X.L., Liu, J., Zhang, D.Y., Chen, X., Song, W.J., and Wu, F.C. (2010) Binding of dicamba to soluble and bound extracellular polymeric substances (EPS) from aerobic activated sludge: A fluorescence quenching study. Journal of Colloid and Interface Science, 345, 442-447.

Prywer, J., and Torzewska, A. (2009) Bacterially induced struvite growth from synthetic urine: Experimental and theoretical characterization of crystal morphology. Crystal Growth & Design, 9, 3538-3543.

Prywer, J., and Torzewska, A. (2010) Biomineralization of struvite crystals by *Proteus mirabilis* from artificial urine and their mesoscopic structure. Crystal Research and Technology, 45, 1283-1289.

Prywer, J., Torzewska, A., and Plocinski, T. (2012) Unique surface and internal structure of struvite crystals formed by *Proteus mirabilis*. Urological Research, 40, 699-707.

Rivadeneyra, A., Gonzalez-Martinez, A., Gonzalez-Lopez, J., Martin-Ramos, D., Martinez-Toledo, M.V., and Rivadeneyra, M.A. (2014) Precipitation of phosphate minerals by microorganisms isolated from a fixed-biofilm reactor used for the treatment of domestic wastewater. International Journal of Environmental Research and Public Health, 11, 3689-3704.

Rivadeneyra, M.A., Gutierrez-Calderon, A., Rivadeneyra, A.M., and Ramos-Cormenzana, A. (1999) A study of struvite precipitation and urease activity in bacteria isolated from patients with urinary infections and their possible involvement in the formation of renal calculi. Urologia Internationalis, 63, 188-192.

Rivadeneyra, M.A., Martin-Algarra, A., Sanchez-Navas, A., and Martin-Ramos, D. (2006) Carbonate and phosphate precipitation by *Chromohalobacter marismortui*. Geomicrobiology Journal, 23, 89-101.

Rivadeneyra, M.A., Perezgarcia, I., and Ramos-Cormenzana, A. (1992) Struvite precipitation

by soil and fresh water bacteria. Current Microbiology, 24, 343-347.

Sadowski, R.R., Prywer, J., and Torzewska, A. (2014) Morphology of struvite crystals as an evidence of bacteria mediated growth. Crystal Research and Technology, 49, 478-489.

Sánchez-Román, M., Rivadeneyra, M.A., Vasconcelos, C., and McKenzie, J.A. (2007) Biomineralization of carbonate and phosphate by moderately halophilic bacteria. FEMS Microbiology Ecology, 61, 273-284.

Schultze-Lam, S., Harauz, G., and Beveridge, T.J. (1992) Participation of a cyanobacterial-S layer in fine-grain mineral formation. Journal of Bacteriology, 174, 7971-7981.

Sheng, G.P., Zhang, M.L., and Yu, H.Q. (2008) Characterization of adsorption properties of extracellular polymeric substances (EPS) extracted from sludge. Colloids and Surfaces B-Biointerfaces, 62, 83-90.

Sikirić, M., Babić-Ivančić, V., Milat, O., Sarig, S., and Füredi-Milhofer, H. (2000) Factors influencing additive interactions with calcium hydrogenphosphate dihydrate crystals. Langmuir, 16, 9261-9266.

Sinha, A., Singh, A., Kumar, S., Khare, S.K., and Ramanan, A. (2014) Microbial mineralization of struvite: A promising process to overcome phosphate sequestering crisis. Water Research, 54, 33-43.

Soares, A., Veesam, M., Simoes, F., Wood, E., Parsons, S.A., and Stephenson, T. (2014) Bio-struvite: A new route to recover phosphorus from wastewater. Clean-Soil Air Water, 42, 994-997.

Song, Y.H., Dai, Y.R., Hu, Q., Yu, X.H., and Qian, F. (2014) Effects of three kinds of organic acids on phosphorus recovery by magnesium ammonium phosphate (MAP) crystallization from synthetic swine wastewater. Chemosphere, 101, 41-48.

Stratful, I., Scrimshaw, M.D., and Lester, J.N. (2001) Conditions influencing the precipitation of magnesium ammonium phosphate. Water Research, 35, 4191-4199.

Taller, A., Grohe, B., Rogers, K.A., Goldberg, H.A., and Hunter, G.K. (2007) Specific adsorption of osteopontin and synthetic polypeptides to calcium oxalate monohydrate crystals. Biophysical Journal, 93, 1768-1777.

Tourney, J., and Ngwenya, B.T. (2009) Bacterial extracellular polymeric substances (EPS) mediate $CaCO_3$ morphology and polymorphism. Chemical Geology, 262, 138-146.

595 Wang, L.L., Wang, L.F., Ren, X.M., Ye, X.D., Li, W.W., Yuan, S.J., Sun, M., Sheng, G.P., Yu,
596 H.Q., and Wang, X.K. (2012) pH dependence of structure and surface properties of
597 microbial EPS. Environmental Science & Technology, 46, 737-744.
598 Wu, J., Kim, K.S., Sung, N.C., Kim, C.H., and Lee, Y.C. (2009) Isolation and characterization
599 of *Shewanella oneidensis* WL-7 capable of decolorizing azo dye Reactive Black 5.
600 Journal of General and Applied Microbiology, 55, 51-55.
601 Xiao, X., Wang, P., Zeng, X., Bartlett, D.H., and Wang, F.P. (2007) *Shewanella psychrophila*
602 sp nov and *Shewanella piezotolerans* sp nov., isolated from west Pacific deep-sea
603 sediment. International Journal of Systematic and Evolutionary Microbiology, 57, 60-65.
604 Xu, M.Y., Guo, J., Cen, Y.H., Zhong, X.Y., Cao, W., and Sun, G.P. (2005) *Shewanella*
605 *decolorationis* sp nov., a dye-decolorizing bacterium isolated from activated sludge of a
606 waste-water treatment plant. International Journal of Systematic and Evolutionary
607 Microbiology, 55, 363-368.
608 Yang, C., Zhang, W., Liu, R.H., Li, Q., Li, B.B., Wang, S.F., Song, C.J., Qiao, C.L., and
609 Mulchandani, A. (2011) Phylogenetic diversity and metabolic potential of activated
610 sludge microbial communities in full-scale wastewater treatment plants. Environmental
611 Science & Technology, 45, 7408-7415.
612 Zhang, F.F., Xu, H.F., Shelobolina, E.S., Konishi, H., Converse, B., Shen, Z.Z. and Roden,
613 E.E. (2015) The catalytic effect of bound extracellular polymeric substances excreted by
614 anaerobic microorganisms on Ca-Mg carbonate precipitation: Implications for the
615 "dolomite problem". American Mineralogist, 100, 483-494.
616 Zhao, J.S., Deng, Y.H., Manno, D., and Hawari, J. (2010) *Shewanella* spp. genomic evolution
617 for a cold marine lifestyle and in-situ explosive biodegradation. PLoS ONE, 5: e9109.
618

619 # Figure captions

620 Figure 1 XRD pattern (a) and FESEM image (b) of the sample obtained in the M-1 medium
621 after 3 d of incubation.

622 Figure 2 FESEM images of the samples synthesized for 3 h in the presence of (a) unseparated
623 liquid culture, (b) deionized water, (c) 0.5% NaCl solution, (d) uninoculated culture
624 medium, (e) native cells and (f) supernatant.

625 Figure 3 XRD patterns of the samples synthesized for 3 h in the presence of (a) unseparated
626 liquid culture, (b) deionized water, (c) uninoculated culture medium, (d) native cells and
627 (e) supernatant.

628 Figure 4 FESEM images of the samples synthesized for 3 h in the (a) LMW component
629 solution and (b) SEPS solution.

630 Figure 5 XPS wide survey scans (a) of the sample synthesized for 3 h in the LMW component
631 solution and high-resolution C 1s (b), O 1s (c) and N 1s (d) spectra of the same sample.

632 Figure 6 FESEM images of the samples synthesized for 3 h in the presence of (a) EPS-free
633 cells and (b) BEPS.

634

635
636
637
638
639
640
641
642
643
644
645
646

Table 1. Composition of the three culture media before and after inoculation

Parameters	Tryptone (g/L)	Yeast extract (g/L)	NaCl (g/L)	Mg^{2+} (mM)	PO_4^{3-} (mM)	NH_4^+ (mM)	pH_i	pH_f*	Struvite mass (mg)*	Transformation efficiency of Mg
M-1	10	5	5	4	4	12	7.0	8.9	76.1	70.5%
M-2	10	5	5	4	4	0	7.0	9.0	73.4	68.0%
M-3	10	5	5	4	0	0	7.0	8.9	74.6	69.1%

647 *：stand for the mean value.

648
649
650
651

652

653

654

655

656

657

658 **Table 2. The bacterial components in solution C**

659

Solution C	Unseparated liquid culture	Suspension of native cells*	Supernatant	LMW component solution	SEPS solution	Suspension of EPS-free cells*	BEPS solution
LMW component	+	-	+	+	-	-	-
SEPS	+	-	+	-	+	-	-
EPS-free Cell	+	+	-	-	-	+	-
BEPS	+	+	-	-	-	-	+

660 *: the native cells or EPS-free cells were suspended by 0.5% NaCl solution with a final volume 45 mL.

661

662

663

664

665

666

667

668

669

670

671

672
673
674
675
676
677
678
679
680
681
682
683 **Table 3. Elemental analysis result of the struvite obtained in the LMW component**
684 **solution (accuracy: 0.2%)**
685

Sample weight (mg)	N (wt %)	C (wt %)	H (wt %)
2.715	5.38	0.94	6.36

686
687
688

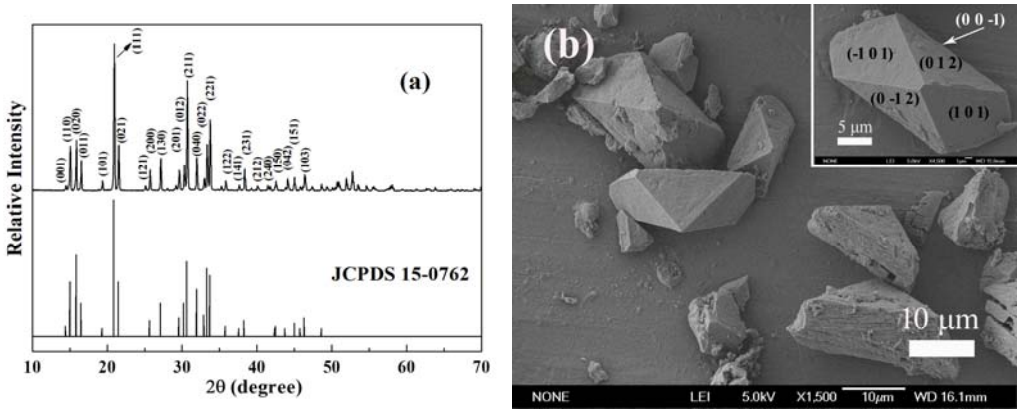

Figure 1

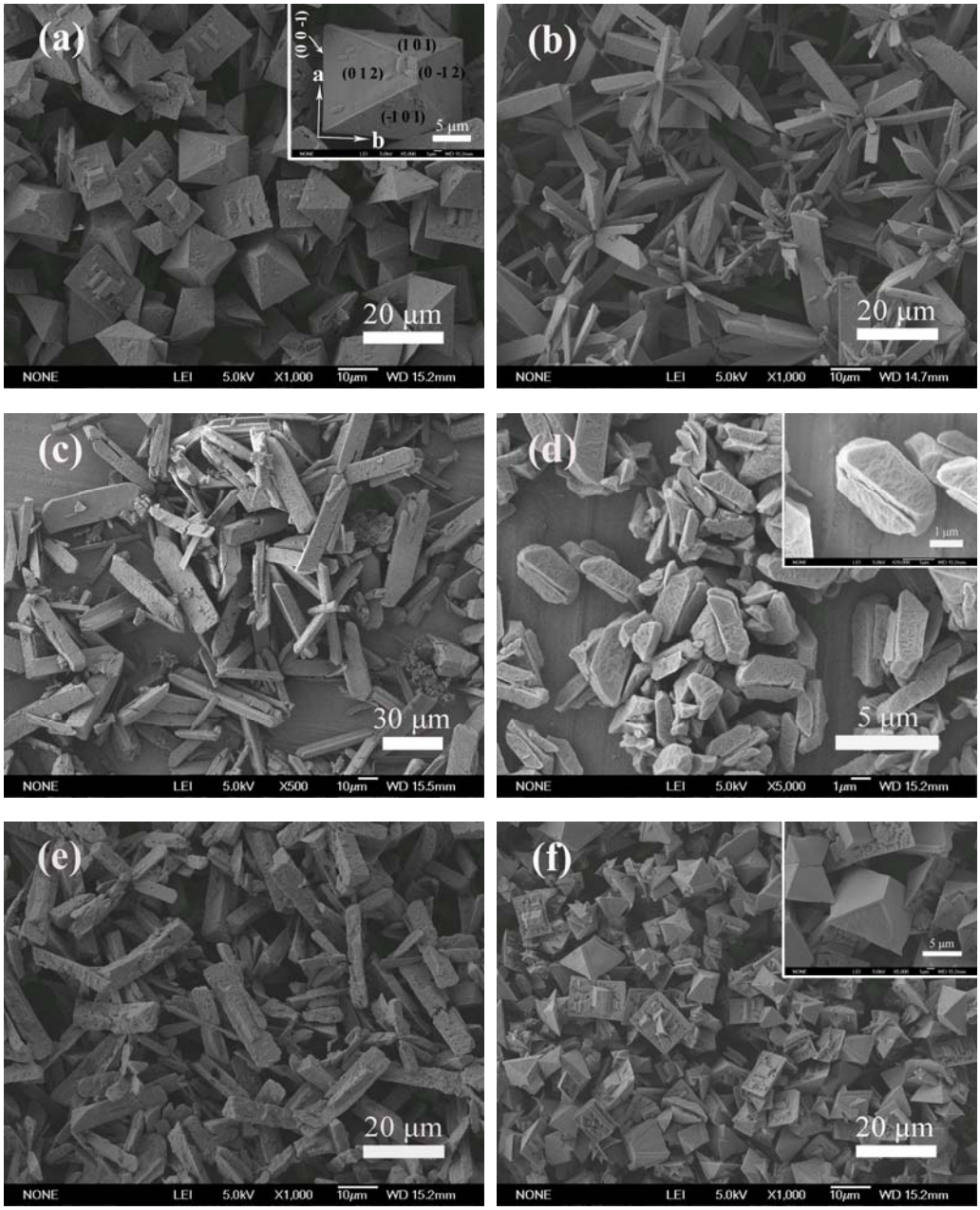

Figure 2

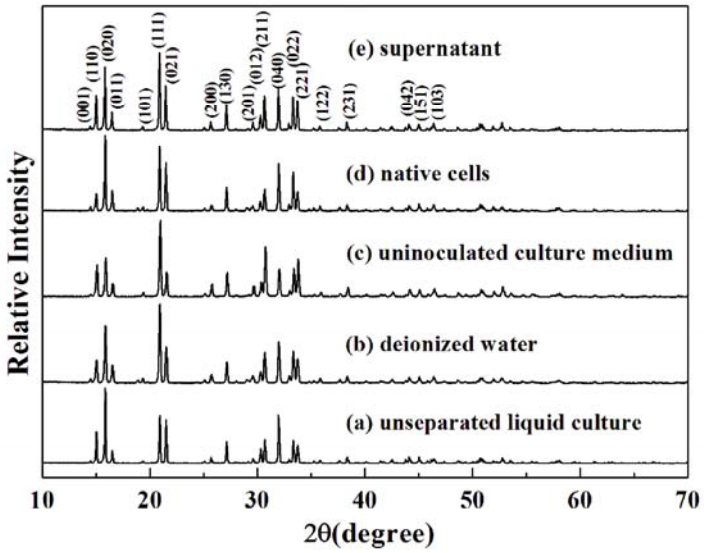

Figure 3

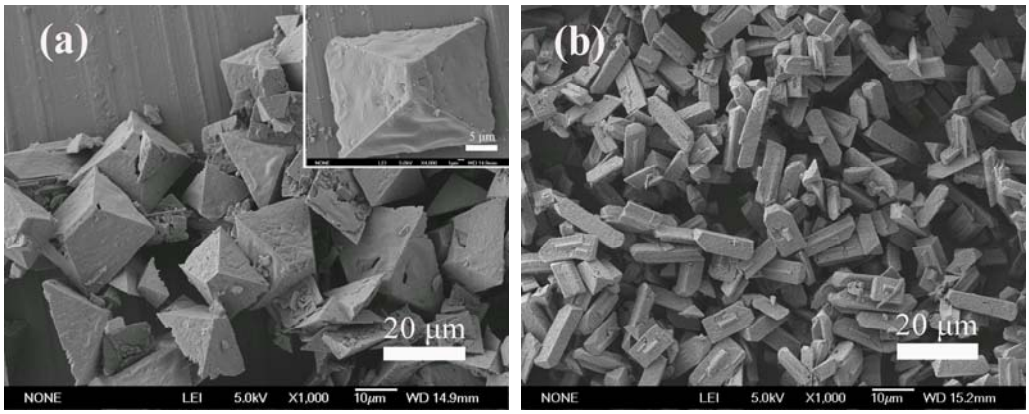

Figure 4

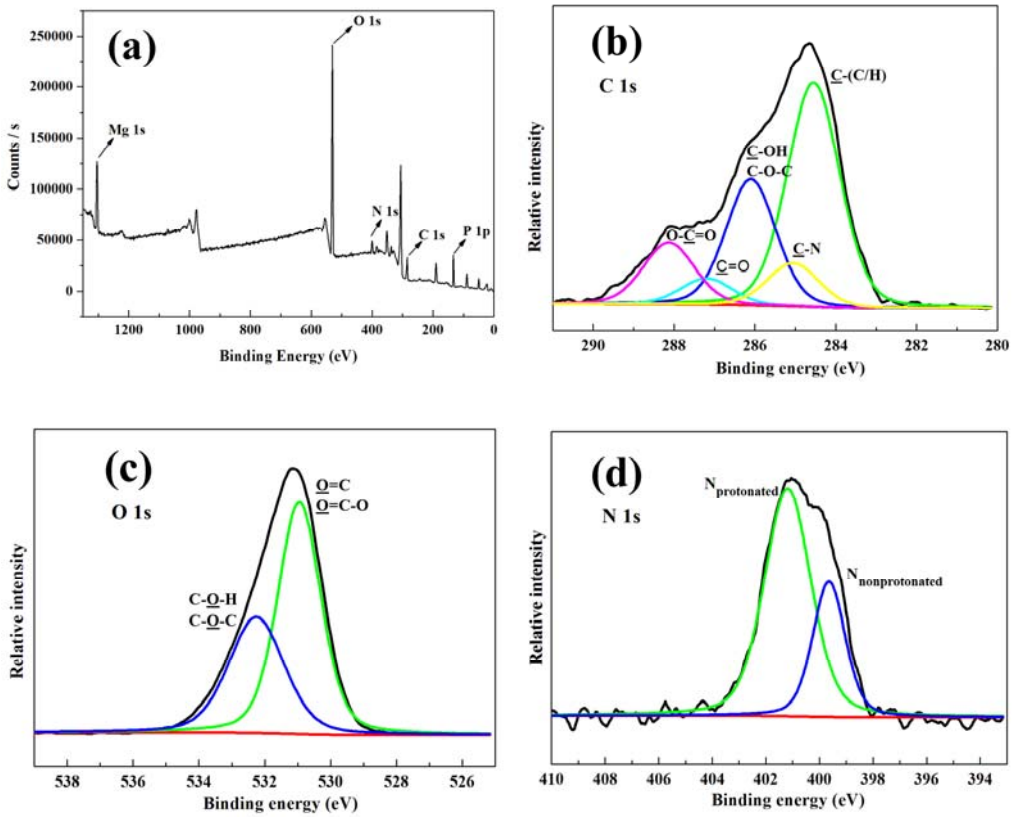

Figure 5

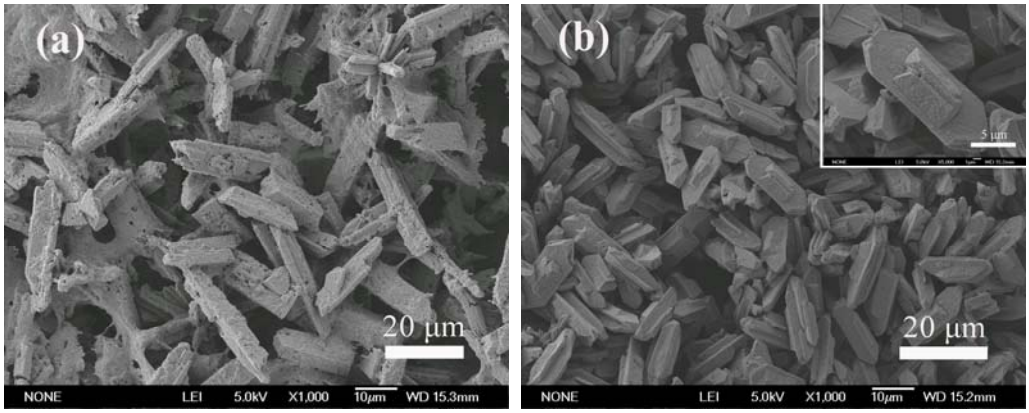

Figure 6